

Wilson, S., Harvey, A. R., Zammit, P. and Zhou, Y. (2017) Enhanced Computational Imaging for Microendoscopy. In: 3D Image Acquisition and Display: Technology, Perception and Applications, San Francisco, CA, USA, 26-29 Jun 2017, JTU5A.19. ISBN 9781557528209 (doi:[10.1364/3D.2017.JTu5A.19](https://doi.org/10.1364/3D.2017.JTu5A.19))

This is the author's final accepted version.

There may be differences between this version and the published version. You are advised to consult the publisher's version if you wish to cite from it.

<http://eprints.gla.ac.uk/146733/>

Deposited on: 11 October 2017

Enhanced Computational Imaging for Microendoscopy

Stuart Henry Wilson, Yongzhuang Zhou, Paul Zammit & Andy R Harvey

School of Physics & Astronomy, The University of Glasgow, Glasgow, UK, G12 8QQ

e-mail address

Abstract: Microendoscope imaging systems suffer from high levels of aberrations, a narrow Field of View and short Depth of Field. We present a technique for enhanced imaging through a microendoscope using a novel computational imaging approach.

OCIS codes: 100.0100, 180.0180.

1. Introduction

1.1. Background

The past fifty years has seen rapid change take place in the biomedical imaging fields, with a push towards minimally invasive, lower toxicity techniques. A surge in active research, relating to this domain, has been taking place within the discipline of microendoscopic imaging. Using techniques such as Optical Biopsy [1], these miniature devices - primarily comprised of Gradient Index (GRIN) optics - have great potential to overcome many of the pitfalls of more invasive characterisation processes (such as Biopsy and the Frozen Section Method.) However, the benefits introduced by using miniaturised optical devices are often hampered by an inherently narrow Field of View (FOV), short Depth of Field (DOF), high levels of intrinsic aberrations and difficulties in navigating the imaging plane through turbid, biological media to the volume of interest. For example, a typical microendoscope with an $NA = 0.5$ has a DOF of less than $1\mu m$ making navigation a particular problem for sub-cellular imaging.

1.2. Computational Imaging

Computational Imaging techniques have already proven disruptive for the biomedical imaging field [2] and provide a possible route for improved imaging in microendoscopy. In their pivotal paper, Dowski and Cathey [3] demonstrated that Wavefront Coding (WC) can be used to digitally recover images with an extended Depth of Field without compromising resolution. The resultant images, however, are clearly degraded by artefacts arising from variations in the encoded point Spread Function (PSF) with defocus. A recent technique, developed by P Zammit et al [4–6], has been shown to overcome such degradations to recover artefact free images with enhanced DOF and 3D ranging.

1.3. Complementary Kernel Matching

Complementary Kernel Matching (CKM) characterises the spatially variant translation of image components as a function of defocus which, in turn, enables the determination of the spatially variant defocus of the scene. Using this defocus map, artefact-free images with an extended DOF can be recovered, along with a two-dimensional defocus and range map of the imaged scene. This has the potential to improve navigation within an in-vivo imaging scenario and overcome some of the limitations mentioned above. For example, considering the same microendoscope as above (with $NA = 0.5$), the application of CKM has the potential to increase the DOF from $1\mu m$ to $10\mu m$ (a factor of ten improvement). This allows for improved navigation and functional sub-cellular imaging.

2. Preliminary Results

Adding a cubic phase distortion to an optical system changes the PSF in a predictable manner. the composite image shown in Figure 1d demonstrates the characteristic cubic PSF with side lobes. This image shows the cubic PSF of a system at three different points along the direction of propagation (z axis). Using the CKM technique, the standard PSFs were recovered (Figure 1b). Figures 1c and 1d show the cubic PSF of the imaging system through the microendoscope device at different points along the z axis.

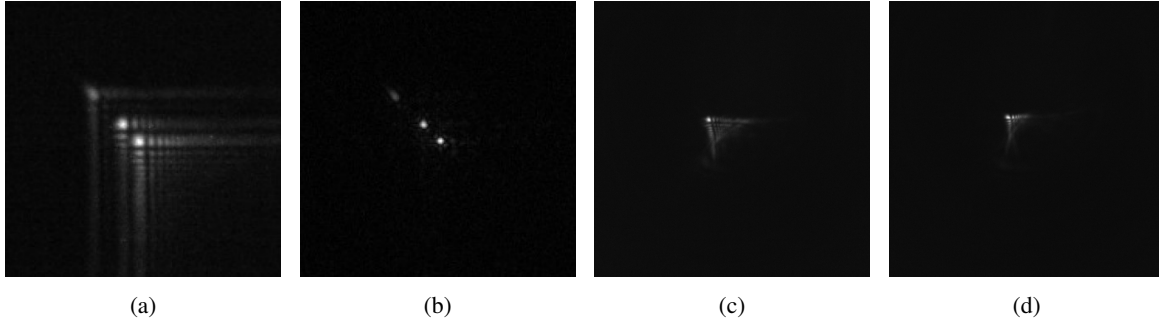


Fig. 1: **(a)** an image of an in-focus particle (PSF) through the microendoscope system. **(b)** an image of the same particle (PSF) at an out of focus z position. **(c)** a composite image of a particle (PSF) z -stack taken without the microendoscope in place. **(d)** the PSFs from **(c)** recovered using the CKM technique.

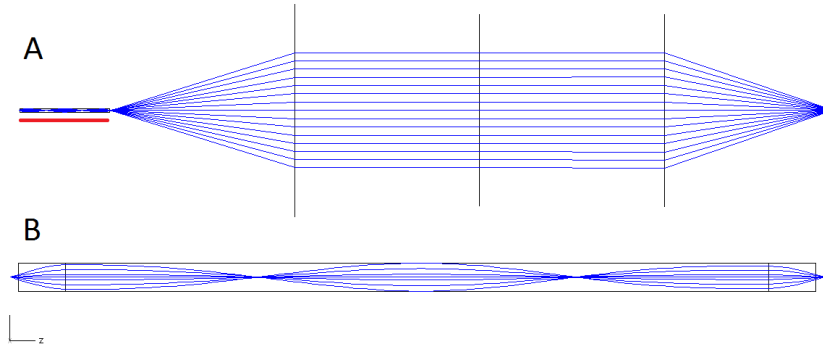


Fig. 2: **A.** Paraxial model of a simple $4f$ system with a microendoscope (highlighted in red). **B.** A zoomed view of the microendoscope model used.

Simulations of a paraxial microendoscope system (Figure 2) were carried out using Zemax Optics Studio to investigate how the introduction of a cubic phase distortion affected the PSFs. Figure 3 demonstrates, as expected, that the PSF varies in xy as a function of z when no phase mask is in place. Adding the phase distortion, however, demonstrates that the resultant cubic PSFs should display the characteristic 'L-shaped' lobes (as demonstrated in Figure 4) in the absence of aberrations.

3. Future Work

Our preliminary results show that there is potential to apply the CKM technique to a microendoscope imaging system. We have demonstrated that the experimental cubic PSFs are significantly degraded compared to the simulated results. It is thought that this may be due to manufacturing processes — or difficulties with aligning the system — which result

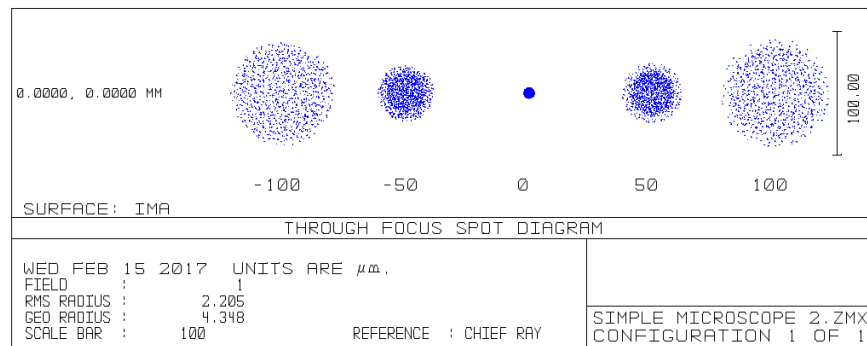


Fig. 3: A series of simulated spot diagrams (through the focal plane) of a microendoscope imaging system. It can clearly be seen that the PSF is a function of system defocus.

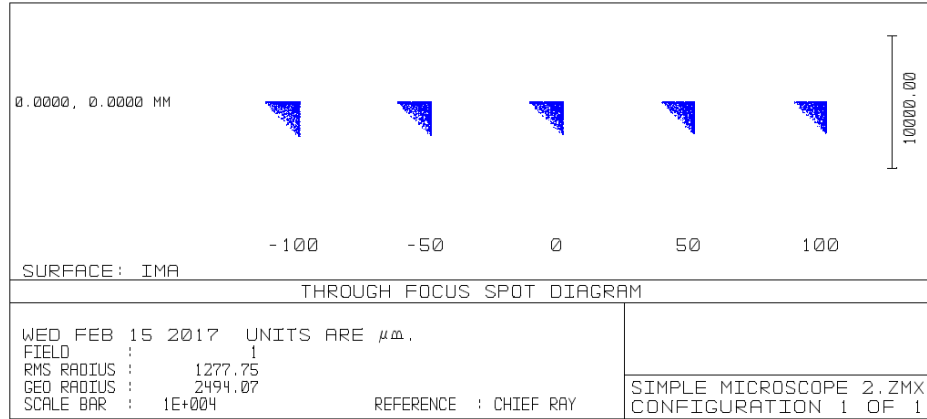


Fig. 4: The same series of simulated spot size diagrams as Figure 3 with a cubic phase mask in place. The series demonstrates that the PSF is unchanged with system defocus.

in increased levels of aberrations.

The ongoing aim of this project is to address the high levels of aberrations in the cubic PSF images (Figures 1c and 1d above) by fully characterising and calibrating the system with the microendoscope in place.

References

1. G. J. Tearney, M. E. Brezinski, B. E. Bouma, S. a Boppart, C. Pitris, J. F. Southern, and J. G. Fujimoto, In vivo endoscopic optical biopsy with optical coherence tomography., *Science*, vol. 276, no. 5321, pp. 20372039, 1997.
2. A. R. Harvey, G. Carles, S. Chen, G. Muyo, J. Downing, N. Bustin, and A. Wood, Computational imaging: the improved and the impossible, *Opt. Syst. Des. 2015 Opt. Des. Eng. VI*, vol. 9626, no. September 23, 2015, p. 96260Q, 2015.
3. E. R. Dowski and W. T. Cathey, Extended depth of field through wave-front coding., *Appl. Opt.*, vol. 34, no. 11, pp. 18591866, 1995.
4. P. Zammit, A. R. Harvey, and G. Carles, Extended depth-of-field imaging and ranging in a snapshot, *Optica*, vol. 1, no. 4, pp. 209216, 2014.
5. A. R. Harvey, Y. Zhou, and P. Zammit, 3D microfluidic particle image velocimetry with extended depth-of-field and a single camera extended depth-of-field and a single camera, *Imaging Appl. Opt.*, 2016, paper JT3A.40
6. P. Zammit, G. Carles, and A. R. Harvey, 3D imaging and ranging in a snapshot, in *Proc. SPIE 9630, Optical Systems Design 2015: Computational Optics*, 2015, vol. 9630, pp. 19.